

Elucidating Intramolecular Vibrational Coupling Mechanisms by Microwave Spectroscopy of Single Vibrationally Mixed Quantum States: Coriolis and Conformer Interactions in Allyl Fluoride

David A. McWhorter and Brooks H. Pate*

Department of Chemistry, University of Virginia, McCormick Road, Charlottesville, Virginia 22901

Received: June 12, 1998; In Final Form: August 24, 1998

We have measured the rotational spectra of several molecular eigenstates of the *cis* and *gauche* asymmetric hydride stretch in order to determine the nature of the weak vibrational interactions observed in these vibrational bands. The rotational spectra are measured using an infrared-microwave double resonance technique based on the Autler–Townes splitting of states in a strong microwave field. From the rotational spectra, we can detect contribution to the eigenstates from both localized structures (*cis* and *gauche*) and states of delocalized structure, or “isomerization states”. Evidence of rotational transitions assigned to isomerization states are observed in from the eigenstates prepared in both the *cis* and *gauche* vibrational band. Furthermore, detection of Coriolis interactions in the *cis* band is observed. However, we do not detect any coupling between states localized around different wells of the potential (i.e., *cis* and *gauche*) suggesting that the molecule is not undergoing isomerization.

Introduction

Statistical theories of unimolecular reactions are based on the assumption of rapid and complete redistribution of vibrational energy.^{1,2} Experiments using both time-domain^{3–5} and frequency-domain^{6–10} methods have been performed to understand the time scale of this process. Both high-resolution spectroscopy and pump–probe spectroscopy can be used to determine the initial rate of intramolecular vibrational energy redistribution (IVR). However, a full understanding of the IVR process requires information about the dynamics following this initial decay. To elucidate the pathway for energy flow a two-color method is required. Several techniques capable of following the subsequent vibrational dynamics have been developed for time-domain studies.^{11–13} In the frequency domain, infrared fluorescence¹⁴ and photodissociation followed by LIF detection of fragments¹⁵ have been used to investigate the long time distribution of vibrational energy. However, these techniques do not contain direct dynamical information.

Recently we have developed a new frequency-domain spectroscopy technique to determine additional dynamical information about the flow of energy in a single molecule.^{16–19} In this technique, we measure the rotational spectrum of single molecular eigenstates in a region of extensive vibrational state mixing. These spectra contain dynamical information in the line shape of the rotational spectrum of a single quantum state.^{16,18} The technique is formally similar to motional narrowing spectroscopy methods used in nuclear magnetic resonance spectroscopy.^{20,21} This technique is applicable to situations where the coupled vibrational states have different characteristic rotational frequencies, as occurs for conformational isomerization.^{19,22} Here we use the rotational spectroscopy of single molecular eigenstates in the high-resolution infrared spectrum of the asymmetric =CH₂ stretch of allyl fluoride (H₂C=CHCH₂F) to determine the origin of the weak vibrational interactions found in the infrared spectrum.²³

The infrared spectrum of allyl fluoride was presented in the

previous paper.²³ We have measured the asymmetric =CH₂ stretch normal-mode spectrum of both the *cis* and *gauche* conformers of the spectrum. The spectra of these two conformers have a qualitatively different appearance. The *cis* spectrum is characterized by very weak vibrational coupling resulting in very slow IVR. The *gauche* spectrum is more typical of the spectra of large polyatomic molecules in the region of the hydride stretch.^{24,25} Much broader spectra are observed with a time scale for initial IVR of 90 ps. We attributed the difference in these spectra to the fact that the local density of *cis* vibrational states is below the threshold for observing extensive IVR. Further, we proposed that the vibrational interactions that are observed in the *cis* spectrum involve the coupling to states with a different conformer character or to weak Coriolis-type interactions. These conclusions are verified by probing the composition of the individual eigenstates using rotational spectroscopy.

Experimental Section

The description of the infrared measurements was presented in the previous paper.²³ We have measured the rotational spectrum of single molecular eigenstates using a high-power microwave technique.¹⁹ In this measurement, the laser is frequency stabilized on a single molecular eigenstate transition through frequency modulation. At another frequency, the laser output is 100% amplitude modulated. This modulation is used for phase sensitive detection of the infrared signal strength. The infrared signal strength is monitored while a high-powered microwave source is scanned. When the microwave frequency is resonant with a transition in the excited vibrational state, a decrease in the infrared signal is observed. These signal dips are caused by the Autler–Townes splitting of states²⁶ as presented previously.¹⁹

The line width of the double-resonance signals is 5 MHz (full width at half-maximum). The relatively broad line width of these signals, compared to the 300 kHz line width we observe in saturation measurements,¹⁷ is beneficiary because we can scan

relative large spectral regions (a few gigahertz) in a reasonable amount of time. Using this double-resonance technique we can measure rotational transitions with a transition moment >0.2 D.¹⁹ The important advantage of this method over saturation-based techniques is that it does not require saturation of the infrared signal.¹⁹ For the allyl fluoride spectrum, we generally do not have sufficient IR power (12 mW) to saturate the IR transitions. With the exception of one of the 3_{21} molecular eigenstates, no saturation is observed for the IR spectrum despite the limited fragmentation of the spectrum by vibrational coupling.

The high-power microwave radiation (20 W) is generated by amplifying the output of a synthesized sweeper (35 mW, HP 8340B) with a traveling wave tube amplifier (Hughes 8000H). This amplifier operates in the 8–18 GHz frequency range. The microwave radiation is coupled into the interaction region of the molecular beam spectrometer using low loss microwave cables and a microwave horn (to broadcast the power onto the molecular beam). This limited tuning range restricts the number of eigenstates we can investigate. Tunable infrared radiation is provided by a color center laser (Burligh Instruments) that is pumped by a Kr⁺ laser (Spectra Physics Model 171). The output of the ion laser is stabilized by an electrooptic technique (ConOptics Model 350-105). Reducing the amplitude noise of the ion pump laser improves the frequency stability of the color center laser and, therefore, the noise when monitoring an infrared signal. In our double-resonance measurements, the noise is approximately 5% of the infrared signal strength.

Prediction of Rotational Transition Frequencies. Rotational spectroscopy is particularly well suited to studies of conformational isomerization.^{18,19,22} The rotational constants of the different conformers can differ significantly so that each conformer has a characteristic spectrum.²⁷ For studies of vibrational interactions at high energy, it is necessary to know both the rotational constants of the different conformers and the rotational constants for vibrational states above the barrier to conformational isomerization. Because these free-rotor-like states have high energies, there have been no previous spectroscopic studies of their rotational spectra. We have used *ab initio* calculations²⁸ to estimate the rotational constants of these states.

The potential energy curve for internal rotation about the C–C single bond in allyl fluoride can be calculated using *ab initio* techniques. In this calculation, the torsional angle is scanned and all other structural parameters are relaxed at each angle in the calculation of the energy. The results of *ab initio* calculations of the torsional potential at two levels of theory²⁹ are compared to experimentally derived potentials^{30,31} in Figure 1 of the previous paper.²³ For allyl fluoride, the experimental and calculated potentials agree to within 1 kcal/mol (350 cm⁻¹).

The wave functions for the torsional energy levels are calculated using a one-dimensional Hamiltonian.³² For this calculation, the torsional potential is expanded in the standard cosine form. The rotational constant for the relative internal motion of the frame and the top is also expanded in a cosine Fourier series.³³ The angular dependence of this rotational constant is calculated using the structural parameters obtained in the *ab initio* calculations. The Hamiltonian is represented in a free-rotor basis set and the matrix representation is diagonalized to obtain the torsional energy levels and their wave functions.³² These wave functions can be characterized as *cis*, *gauche*, or torsionally delocalized. The torsionally delocalized wave functions are found over the barrier to isomerization and have significant probability in both the *cis* and *gauche* regions of the potential. At increasing energy, these eigenfunctions more

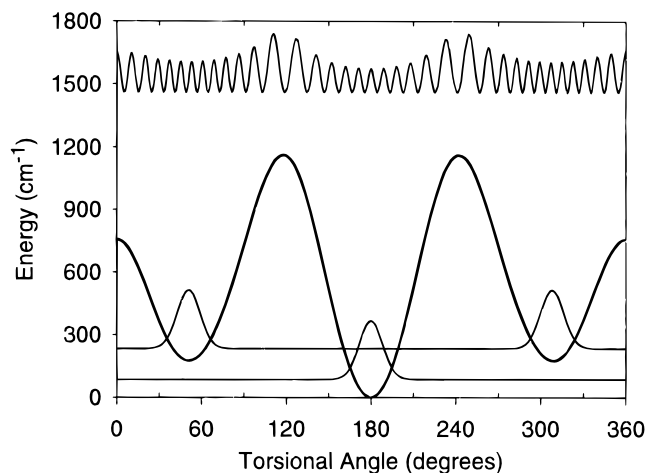


Figure 1. Superimposed on the torsional potential of allyl fluoride are the wave function probabilities of the three types of states that are involved in the vibrational energy redistribution dynamics. The lowest energy probability curve represents the ground torsional state of the *cis* conformer. The ground-state wave function probability of the *gauche* conformer has equal probability in each of the double wells. The torsionally delocalized wave function, seen at the top of the figure, has an energy that exceeds the barrier to isomerization and has nearly equal probability over the entire torsional potential. This torsional potential was computed at the HF/6-311G** level of theory. The energies were calculated at 10° increments except in the region of the *gauche* conformer (46°–57°) where points were calculated every 1°. The bottom of the *cis* well ($\phi = 180^\circ$) has been set to 0 cm⁻¹.

closely resemble free-rotor wave functions. These types of torsional eigenfunctions are illustrated in Figure 1. The torsional potential seen in Figure 1 was calculated via *ab initio* methods at the HF/6-311G** level of theory. We have found that this level of theory accurately predicts the shape of the torsional potentials, the values of the rotational constants (for both stable conformers and excited states), and the structures of several molecular systems that we have investigated.³⁴

We estimate the rotational constants for each of the torsional eigenfunctions by calculating the expectation value of the rotational constant. This method corresponds to including the effects of the angular dependence of the moment of inertia but neglects any Coriolis-like interactions caused by the internal angular momentum generated by the internal rotation.^{30,35} To perform this calculation, we fit the angular dependence of the rotational constant to a Fourier cosine series and use this expansion in the expectation value calculation. We have tested this method for the low-lying torsional states by comparing the calculated rotational constants with experimental values.³⁶ In addition, we scale the $\nu = 0$ results from the *ab initio* calculation to the experimental determination. The actual calculated results (i.e., unscaled) and the experimental results are given in Table 1. The comparison to experiment for the *cis* and *gauche* torsional states is shown in Figure 2. Overall, the agreement is very good with errors of less than 1% (after scaling). For the *cis* conformer we recover all trends in the changes of the rotational constants with torsional excitation. The agreement for the *gauche* torsional states is not as good. The *gauche* torsional states occur in near-degenerate pairs of symmetric and antisymmetric states separated by the tunneling splitting. These near-degenerate pairs of states are most susceptible to Coriolis effects and this may be the origin of the discrepancy.

Using this calculational approach we can also estimate the rotational constants of the delocalized torsional states. Additionally, we calculate the expectation value of the dipole moment components for each state. Experimental dipole moments are

TABLE 1: Calculated and Measured Rotational Constants and Dipole Moments for Cis and Gauche Allyl Fluoride States in Ground and Torsionally Excited States (Indicated by the Number of Quanta in the Torsion Vibration) and the Rotational Constants and Dipole Moments Calculated for a Delocalized State^a

	cis experimental ^b	ab initio ^c	gauche experimental ^b	ab initio ^c
$\nu = 0$				
A	17 236.63	17 810	27 720.34	29 121
B	6 002.91	6 025	4 263.62	4 311
C	4 579.82	4 632	4 131.98	4 150
μ_a (D)	0.742 ± 0.008	0.697	1.595 ± 0.006	1.596
μ_b (D)	1.601 ± 0.011	1.763	0.908 ± 0.012	0.874
μ_c (D)			0.623 ± 0.014	0.908
$\nu = 1$				
A	17 256.69	17 866	27 690.86	29 093
B	5 967.08	5 990	4 271.79	4 328
C	4 580.96	4 632	4 148.65	4 155
μ_a (D)		0.718		1.585
μ_b (D)		1.751		0.797
μ_c (D)		0		0.921
$\nu = 2$				
A	17 284.73	17 927	27 702.64	29 150
B	5 930.46	5 954	4 278.64	4 343
C	4 581.28	4 628	4 162.44	4 156
μ_a (D)		0.741		1.574
μ_b (D)		1.736		0.646
μ_c (D)		0		0.904
delocalized level		ab initio ^c		
A		24 643		
B		4 903		
C		4 346		
μ_a (D)		1.299		
μ_b (D)		1.205		
μ_c (D)		0		

^a Values in MHz except where noted. ^b Reported in ref 36. ^c Values averaged over the torsional wave function. Ab initio calculations were performed at the HF/6-311G** level of theory.

available only for the ground torsional state of each conformer,³⁶ and our calculated values are in good agreement. These results are also given in Table 1. From these calculations we can determine the rotational transition frequency as a function of the torsional quantum state. A calculation of the $2_{02}-1_{01}$ transition frequency is shown in Figure 3. This result demonstrates the utility of microwave spectroscopy for determining the torsional character of mixed vibrational states. There is a rapid transition between the rotational frequencies characteristic of the two conformers and the values estimated for the torsionally delocalized states. Furthermore, these transition frequencies are well separated. On the basis of our previous measurement of the rotational constant distribution of propynol at 3330 cm^{-1} ,¹⁷ we expect that vibrational excitation in normal modes other than the torsional mode will produce only small changes to the characteristic frequencies. In Table 2 we give the rotational transitions for cis, gauche, and delocalized torsional states near the tuning range of our high-power microwave source.

Rotational Spectroscopy of Single Vibrationally Mixed Eigenstates. In the next few sections we present results obtained for the rotational spectroscopy of single molecular eigenstates in the cis and gauche asymmetric $=\text{CH}_2$ stretch spectrum. For the cis conformer, where the intramolecular vibrational coupling is sparse, we are able to determine the origin of the weak interactions for several perturbations. We have identified both perpendicular Coriolis-type interactions ($\Delta K_a = -1$) and vibrational interactions between the cis bright state and vibrational states with a free-rotor torsional character. In both cases

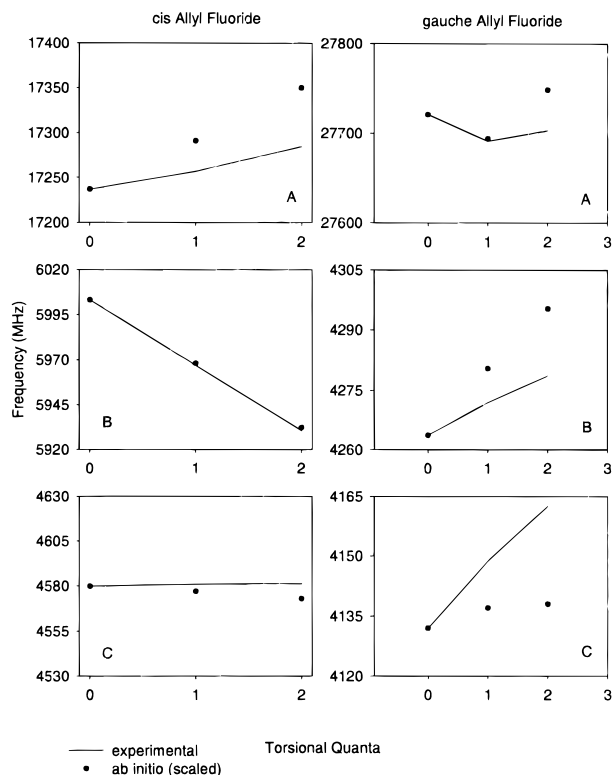


Figure 2. Shown here is the comparison between experimental results and scaled ab initio calculations for the rotational constants of allyl fluoride as the number of quanta of energy in the C-C torsion increases.

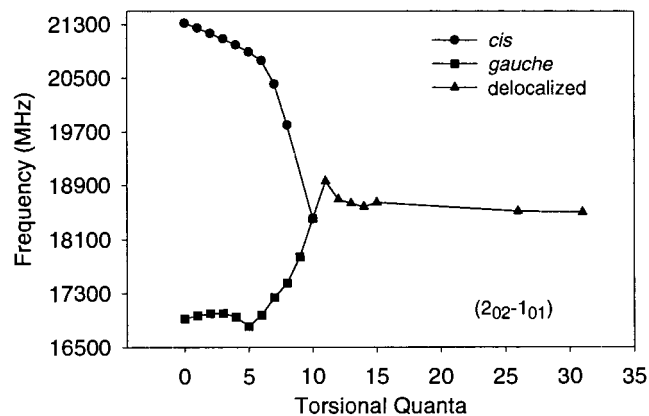


Figure 3. From the calculation of the rotational constants of the molecule as the torsional excitation increases, we are able to estimate the rotational transition frequencies expected for different torsional levels. Shown here is a rapid transition between the rotational frequencies characteristic of the two conformers and the rotational frequencies expected for the torsionally delocalized states for the $2_{02}-1_{01}$ rotational transition.

these interactions are weak, with matrix elements of approximately 80 MHz. By probing eigenstates in the gauche spectrum, we find a similar size for the coupling strength between gauche states and states with free-rotor torsional functions. Searches for the presence of a gauche conformer contribution to the eigenstates in the cis spectrum or a cis contribution to eigenstates in the gauche spectrum, failed to detect any evidence for coupling between these types of states.

Transitions Corresponding to the IR Spectrum. To test the sensitivity of the upper state rotational spectroscopy technique, we have measured transitions between eigenstates appearing in the cis and gauche spectra of the asymmetric $=\text{CH}_2$ stretch.²³ These transitions occur between single eigenstates

TABLE 2: Predicted Rotational Transition Frequencies for Cis, Gauche, and Delocalized States of Allyl Fluoride ($J = 1, 2$, or 3) That Fall near the TWTA Range

conformer	transition	frequency (MHz)	conformer	transition	frequency (MHz)		
cis ^a			delocalized ^c				
$J = 1$	$1_{01}-0_{00}$	10 583	$J = 1$	$2_{12}-1_{11}$	18 030		
	$1_{10}-1_{01}$	12 657		$2_{02}-1_{01}$	18 587		
	$2_{12}-1_{11}$	19 742		$2_{11}-1_{10}$	19 169		
	$2_{02}-1_{01}$	21 039		$1_{11}-1_{01}$	19 275		
	$1_{11}-0_{00}$	21 817		$1_{10}-1_{01}$	19 844		
	$2_{11}-1_{10}$	22 589		$1_{11}-0_{00}$	28 574		
	$J = 2$	$2_{11}-2_{02}$		14 207	$1_{10}-0_{00}$	29 144	
		$J = 3$		$4_{13}-3_{22}$	13 250	$2_{12}-2_{02}$	18 718
	$3_{31}-4_{22}$			15 730	$2_{11}-2_{02}$	20 427	
	$3_{12}-3_{03}$			16 759	$J = 3$	$4_{04}-3_{12}$	15 750
	$2_{20}-3_{03}$			16 788		$3_{13}-3_{03}$	17 906
	$3_{30}-4_{23}$			17 576		$3_{22}-4_{13}$	18 668
$3_{03}-2_{12}$	21 310		$3_{21}-4_{13}$	18 730			
$3_{13}-2_{12}$	29 537		$4_{04}-3_{13}$	19 168			
gauche ^b	$J = 1$		$2_{12}-1_{11}$	16 660		$3_{12}-3_{03}$	21 323
			$2_{02}-1_{01}$	16 791		$3_{22}-4_{14}$	24 363
		$2_{11}-1_{10}$	16 923	$3_{21}-4_{14}$		24 425	
	$J = 2$	$1_{11}-1_{01}$	23 457	$3_{13}-2_{12}$		27 037	
		$1_{10}-1_{01}$	23 588	$3_{03}-2_{02}$	27 849		
		$2_{12}-2_{02}$	23 326	$3_{22}-2_{21}$	27 900		
	$J = 3$	$2_{11}-2_{02}$	23 721	$3_{21}-2_{20}$	27 950		
		$4_{04}-3_{13}$	10 445	$3_{12}-2_{11}$	28 745		
		$3_{13}-3_{03}$	23 131	$2_{21}-3_{12}$	29 079		
		$3_{12}-3_{03}$	23 920	$2_{20}-3_{12}$	29 092		
		$3_{13}-2_{12}$	24 989				
		$3_{03}-2_{02}$	25 184				
$3_{22}-2_{21}$	25 188						
$3_{21}-2_{20}$	25 191						
$3_{12}-2_{11}$	25 384						

^a $\mu_a = 0.74$ D, $\mu_b = 1.6$ D (see ref 36). ^b $\mu_a = 1.59$ D, $\mu_b = 0.9$ D, $\mu_c = 0.62$ D (see ref 36). ^c $\mu_a = 1.299$ D, $\mu_b = 0.46$ D (rotational constants and dipole moments calculated from delocalized wave function expectation value).

that are known to have bright state character. On the basis of the dipole moment components along the principal axes and rotational transitions predicted to lie in the available tuning range, we have concentrated on the b-type $K_a = 0-1$ Q-branch transitions of the cis conformer and the a-type $J = 2-1$ transitions of the gauche conformer.

The 3_{03} and 3_{12} IVR multiplets for the cis conformer are shown in Figure 4. Because this spectrum is so sparse, we expect that the rotational spectrum of the 3_{03} eigenstate will mimic the 3_{12} IVR multiplet.³⁷ Stabilizing the laser on the 3_{03} eigenstate, we scanned the region of the $3_{12}-3_{03}$ rotational transition. We have observed three of the four eigenstates that appear in the 3_{12} spectrum. The transition frequencies are reported in Table 3. As expected, the transition at 16844 MHz, which accesses the strong transition in the 3_{12} spectrum, is stronger than the other two observed signals. Because the double-resonance technique does not require IR saturation, we can also investigate the rotational spectra of the weak transitions in the 3_{12} multiplet. For the three most intense molecular eigenstates in the 3_{12} spectrum we observe a single rotational transition to the most intense 3_{03} state appearing in the infrared spectrum. We have measured the rotational spectra of a few molecular eigenstates in the 1_{01} IVR multiplet of the gauche spectrum. These results will be discussed more fully below, however, for these eigenstates we observe rotational transitions near the characteristic frequency for a gauche $2_{02}-1_{01}$ rotational transition. Furthermore, the eigenstates accessed in the 2_{02} region of the spectrum also appear in the infrared spectrum. These

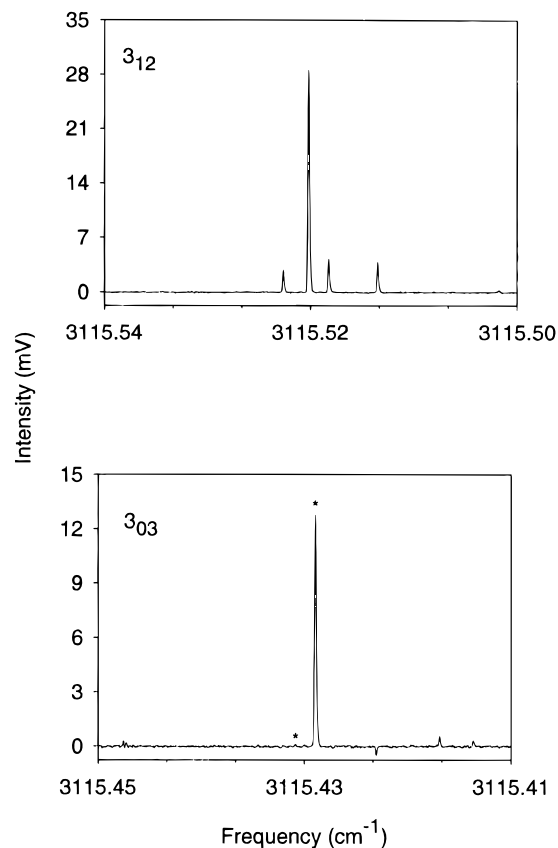


Figure 4. Shown here are the 3_{12} and 3_{03} IVR multiplets of the cis conformer (see ref 23). We measured the rotational spectrum of the three most intense (out of four) 3_{12} eigenstates (the three lower energy states) and also the most intense 3_{03} eigenstate. The two 3_{03} eigenstates have been marked for clarity. From each of the three 3_{12} eigenstates, we observe a rotational transition to the most intense 3_{03} eigenstate seen in the lower panel. From the 3_{03} eigenstate we observe rotational transitions to the three lower energy 3_{12} eigenstates seen in the top panel.

preliminary measurements indicate that we have sufficient sensitivity to observe cis and gauche contributions to single molecular eigenstates.

Detection of Perpendicular Coriolis Interactions. The slow IVR rates observed in the cis allyl fluoride spectra are comparable to the rates of conformational isomerization that we measured in 2-fluoroethanol¹⁹ and to Coriolis-like IVR that we observed in the O-H stretch of propynol.³⁸ Using microwave spectroscopy we can probe whether the weak interactions observed in the cis spectrum are attributable to conformer coupling or Coriolis interactions. For example, we can probe for Coriolis interactions using the level scheme depicted in Figure 5. In this measurement we stabilize the laser on a single eigenstate of the 3_{21} IVR multiplet of the cis spectrum. This multiplet is shown in Figure 6. No rotational transitions of the cis conformer involving the 3_{21} rotational level are predicted to lie in our microwave tuning range (see Table 2). However, if the weak interactions involve perpendicular Coriolis coupling ($\Delta K_a = \pm 1$), then we will observe transitions in the 16759 MHz range ($3_{12}-3_{03}$ transitions) or the 17576 MHz region ($3_{30}-4_{23}$ transitions).

We have measured the rotational spectra of the two molecular eigenstates indicated in Figure 6. We have detected three rotational transitions for each eigenstate with the frequencies reported in Table 3. These transitions access the same molecular eigenstates and from the frequency shifts we can determine that

TABLE 3: Observed Rotational Transitions from the Cis and Gauche Eigenstates

IVR multiplet ($J_{K_a K_c}$)	frequency ^a (cm ⁻¹)	relative frequency (MHz)	rotational transitions ^b (MHz)	assignment ($J'_{(K_a K_c)} \leftarrow J''_{(K_a K_c)}$; conformer)	
cis	1 ₀₁	3113.700	0	18 069 ^a	2 \leftarrow 1, $\Delta K_a = 0$; delocalized
		3113.689	-329	18 399 ^a	2 \leftarrow 1, $\Delta K_a = 0$; delocalized
	1 ₁₁	3113.727	0	17 310 ^b	2 \leftarrow 1, $\Delta K_a = 0$; delocalized
		3113.718	-275	17 807 ^c	2 \leftarrow 1, $\Delta K_a = 0$; delocalized
	1 ₁₀	3113.640		17 585 ^b	2 \leftarrow 1, $\Delta K_a = 0$; delocalized
				18 081 ^c	2 \leftarrow 1, $\Delta K_a = 0$; delocalized
				17 845 ^d	2 \leftarrow 1, $\Delta K_a = 0$; delocalized
	2 ₁₁	3113.638	-58	18 213	2 \leftarrow 1, $\Delta K_a = 0$; delocalized
		3115.153	0	17 905 ^d	2 \leftarrow 1, $\Delta K_a = 0$; delocalized
	3 ₀₃	3115.145	-239	18 025 ^e	1 \leftarrow 2, $\Delta K_a = 0$; delocalized
		3115.429	-	17 783 ^e	1 \leftarrow 2, $\Delta K_a = 0$; delocalized
	3 ₁₂	3115.511	0	16 643 ¹	3 ₁₂ \leftarrow 3 ₀₃ ; cis
			-62	16 783 ²	3 ₁₂ \leftarrow 3 ₀₃ ; cis
	3 ₂₁	3115.509	0	16 844 ³	3 ₁₂ \leftarrow 3 ₀₃ ; cis
			-202	16 844 ³	3 ₀₃ \leftarrow 3 ₁₂ ; cis
			0	16 783 ²	3 ₀₃ \leftarrow 3 ₁₂ ; cis
0			16 643 ¹	3 ₀₃ \leftarrow 3 ₁₂ ; cis	
gauche	3115.476		16 756 ^f	3 ₀₃ \leftarrow 3 ₁₂ ; cis	
			16 876 ^g	3 ₀₃ \leftarrow 3 ₁₂ ; cis	
			17 055 ^h	3 ₀₃ \leftarrow 3 ₁₂ ; cis	
			16 522 ^f	3 ₀₃ \leftarrow 3 ₁₂ ; cis	
			16 644 ^g	3 ₀₃ \leftarrow 3 ₁₂ ; cis	
			16 821 ^h	3 ₀₃ \leftarrow 3 ₁₂ ; cis	
1 ₀₁	3099.15	0	16 807 ¹	2 \leftarrow 1, $\Delta K_a = 0$; gauche	
		-1544	17 346 ²	2 \leftarrow 1, $\Delta K_a = 0$; delocalized	
	3099.10		16 983 ^a	2 \leftarrow 1, $\Delta K_a = 0$; gauche	
			17 994 ^b	2 \leftarrow 1, $\Delta K_a = 0$; delocalized	
	3099.09		17 143 ^a	2 \leftarrow 1, $\Delta K_a = 0$; gauche	
			18 154 ^b	2 \leftarrow 1, $\Delta K_a = 0$; delocalized	
	2 ₀₂	3099.12	0	17 346 ²	1 \leftarrow 2, $\Delta K_a = 0$; delocalized
		3099.10	-539	16 807 ¹	1 \leftarrow 2, $\Delta K_a = 0$; gauche
			17 955	1 \leftarrow 2, $\Delta K_a = 0$; delocalized	

^a These absolute values are taken as the relative position from the start of an infrared scan. The starting frequency of the scan is given by the wavemeter (accurate to ± 0.01 cm⁻¹). The values in this column are given more significant figures when several lie closer than 0.01 cm⁻¹ apart. ^b Common superscript letters indicate that the transitions access the same molecular eigenstate. Common superscript numerals indicate identical transitions (e.g., two separate transitions assigned to 3₀₃ \rightarrow 3₁₂ and 3₁₂ \rightarrow 3₀₃ would be given the same superscript numeral).

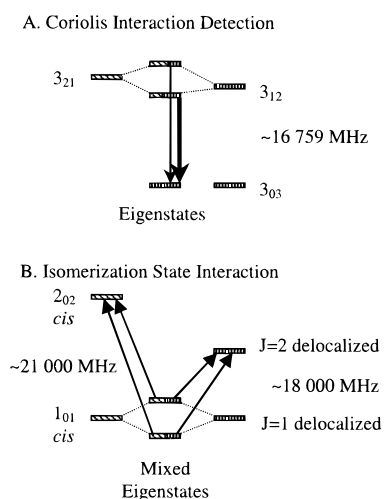


Figure 5. Detection schemes for the observation of Coriolis interaction and isomerization state interaction are given. For the detection of Coriolis interaction in the cis vibrational band, we stabilize the laser to an eigenstate of the 3₂₁ IVR multiplet and measure the rotational spectrum in the frequency range predicted for 3₁₂ \rightarrow 3₀₃ and 3₃₀ \rightarrow 4₂₃ rotational transitions. The idea is the same for detecting isomerization state interactions. Depicted in the bottom panel is a measurement of an eigenstate of the 1₀₁ IVR multiplet. Any $J = 1$ transitions that are observed in the 18 GHz frequency region can be assigned to transitions of the state with torsionally delocalized character (see Table 2).

the transitions reach eigenstates at lower energy. This result and the fact that the transitions are very close to the predicted 3₁₂ \rightarrow 3₀₃ cis rotational transition allow us to assign this weak interaction to a Coriolis-like interaction between two vibrational

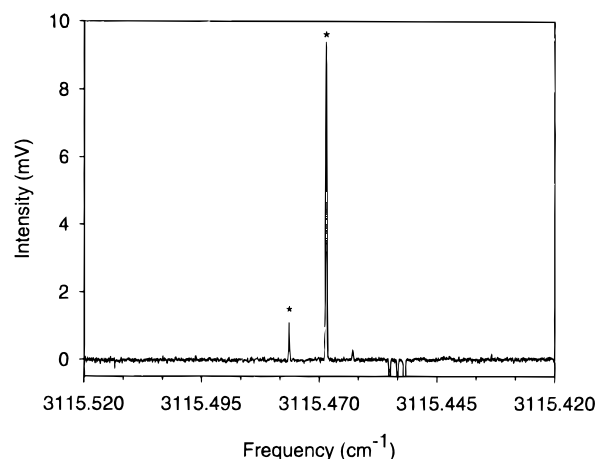


Figure 6. The 3₂₁ IVR multiplet of the cis vibrational band is seen here. We have measured the rotational spectra of the two eigenstates marked by asterisks. These eigenstates have rotational transitions in the 16522–17055 MHz region that we assign to (3₁₂ \rightarrow 3₀₃)-like transitions resulting from Coriolis coupling between the 3₂₁ bright state and a 3₁₂ bath state of the cis conformer (see Figure 5).

states with cis torsional character. From a Lawrence–Knight^{39,40} analysis of the spectrum, the matrix element for this interaction is 73 MHz.

The rotational transitions from the weaker infrared transition are substantially stronger. We can gauge the transition strength from the fact that Autler–Townes dips are observed for the eigenstate with a weak IR intensity, but narrow saturation signals are observed for the eigenstate with the strong IR intensity. To observe an Autler–Townes double-resonance signal, the rota-

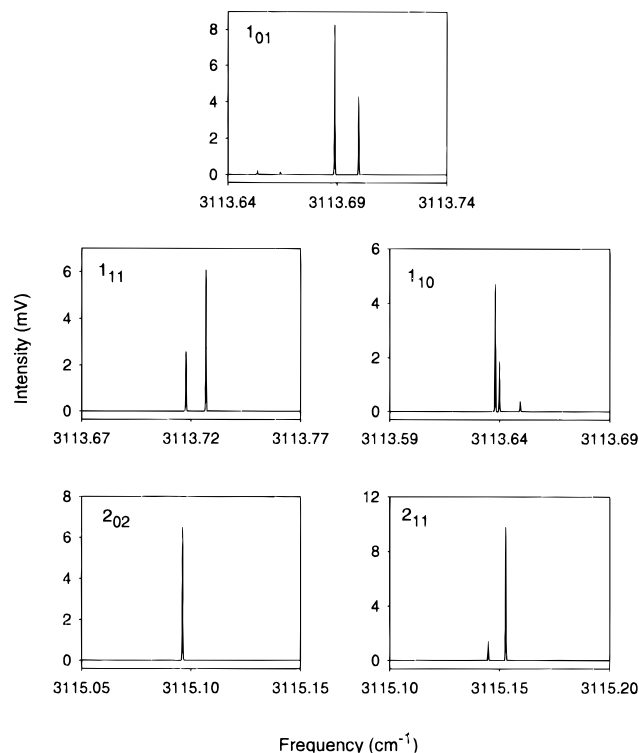


Figure 7. The $J = 1$ and $J = 2$ IVR multiplets of the cis vibrational band that we have used for upper state microwave spectroscopy are shown. For all of the $J = 1$ eigenstate sets and for the 2_{11} states, we observe rotational transitions characteristic of torsionally delocalized states. No transitions were observed from the lone 2_{02} eigenstate.

tional transition strength must be ~ 0.1 D in order to split the interacting states beyond our infrared resolution of 6 MHz. With this transition strength, the saturation signals would be strongly power broadened.⁴¹ The observation of narrow saturation signals, therefore, indicates a much weaker transition moment to the “dark” eigenstates ~ 17 GHz lower in energy. This result just reflects the fact that the eigenstate with strong IR intensity has a dominant contribution from the cis 3_{21} vibrational bright state. This contribution is inactive in the rotational spectrum. Conversely, the eigenstate that has the weak IR intensity must have a dominant contribution from the coupled 3_{12} cis bath state. Because the measurements are obtained through different double-resonance mechanisms (saturation vs Autler–Townes dip), it is difficult to quantitatively determine the relative transition strengths from the two eigenstates.

Detection of Coupling to Torsionally Delocalized States.

To test for the presence of coupling between the cis asymmetric $=\text{CH}_2$ stretch bright state and vibrational states with different torsional character (either gauche or delocalized torsional wave functions), we have investigated the rotational spectra of the $J = 1$ and $J = 2$ molecular eigenstates in the cis IR spectrum. A gauche contribution to the molecular eigenstate is expected to generate rotational transitions in the 16.6–16.9 GHz region and a delocalized transition in the 18.0–19.2 GHz region (see Table 2). The level structure for coupling between the cis bright state and a vibrational state with torsionally delocalized character is illustrated in Figure 5. The $J = 1$ and $J = 2$ cis IVR multiplets that we have used in our study of upper state rotational transitions are shown in Figure 7. For all three of the $J = 1$ eigenstate sets and the 2_{11} states we observe rotational transitions characteristic of torsionally delocalized states. The transition frequencies are reported in Table 3. Because we measure the transitions from two eigenstates of the IR spectrum, we confirm

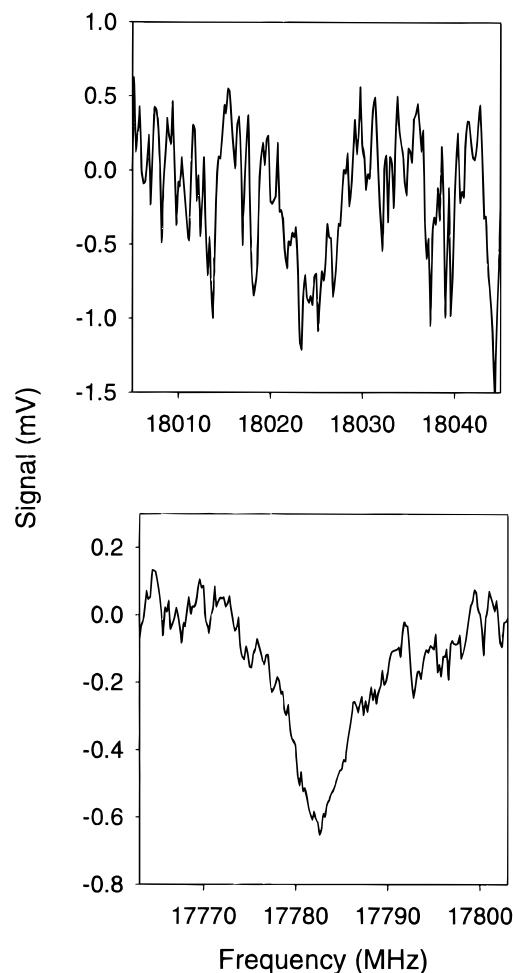


Figure 8. Shown here are the double-resonance signals observed from the 2_{11} eigenstates seen in Figure 7. The infrared transition to the eigenstate measured in the top panel is 7 times the intensity of the infrared transition to the eigenstate measured in the bottom panel. As seen, the rotational transition of the eigenstate of the top panel is about 6.5 times weaker than the transition seen in the bottom panel.

that the final states of the $J = 1$ transitions lie higher in energy and the final states of the $J = 2$ transitions lie lower in energy, as expected for a $J = 2-1$ rotational transition.

Again, we observe complementarity in the rotational spectrum. For example, the double-resonance signals for the two molecular eigenstates in 2_{11} IVR multiplet are shown in Figure 8. For the Autler–Townes double-resonance mechanism, the percentage change in the IR signal is proportional to the square of the rotational transition moment. Also, the intensities in the IR spectrum are proportional to the magnitude squared of the cis bright-state contribution.^{24,25} Therefore, for a simple two-state interaction, the ratios of the signal decrease in the double-resonance spectrum should complement the ratio of the IR intensities. The IR intensity ratio is approximately 1:7 and the percentage signal decreases are 23% and 3.5% for the weak IR and strong IR eigenstates, respectively. This result indicates that the perturbation in the 2_{11} IR spectrum can be treated as a two-state interaction. The coupling matrix elements that can be assigned to the cis bright-state/delocalized state interactions in the $J = 1$ and $J = 2$ spectra range from 74 to 157 MHz.

There are two features of these measurements that should be noted. First of all, many of the observed transition frequencies that we are assigning to vibrational states with torsionally delocalized character lie below 18 GHz and are lower than predicted by our expectation value calculation. In the rotational

spectrum of single eigenstates of 2-fluoroethanol we also found that the observed frequencies for these transitions were lower than predicted.¹⁹ This result could be caused by a dynamic effect. In our averaging, we assume that the molecule assumes a “compact” structure when it is in regions of the conformer minima. However, these torsionally delocalized states correspond to essentially free-rotor motion. During this motion the molecule may remain slightly “expanded” during the full torsional cycle. This effect would decrease the rotational frequencies for these states.

Second, the fact that we observe coupling to torsionally delocalized states in 4 of the 5 $J = 1$ and $J = 2$ IVR multiplets of the cis conformer is statistically unlikely (no rotational transitions were observed from the 2_{02} eigenstate we measured). As reported in the previous study, the density of torsionally delocalized states is only about 1.5 states/cm⁻¹.²³ Because we expect that there should be no conservation of K_a in this type of interaction, the rovibrational density of these states at $J = 1$ is 4.5 states/cm⁻¹. Therefore, the mean level spacing is 6662 MHz. The rotational constants for these states are sufficiently different from the cis bright state constants that each measurement can be treated as statistically independent. With such a low density, it is unlikely that we would observe this type of interaction as frequently as we do.

If we assume that the uncoupled vibrational states are randomly distributed, then we can use Poisson statistics to estimate the probability of observing this type of interaction. Since the matrix elements are so weak, we assume that we can only observe interaction with these states if they lie within ± 600 MHz of the bright-state. This value is chosen based on intensity considerations: For a two-state interaction with a coupling matrix element of 100 MHz, the interaction with a state 600 MHz away produces two eigenstates observable in the infrared spectrum. The less intense transition will have intensity about 3% of the intensity of the more intense transition. The probability of having a delocalized state lie within 600 MHz of the bright state is

$$P = Z \int_0^{s_{\max}} e^{-s/\langle s \rangle} ds \approx \frac{2s_{\max}}{\langle s \rangle}; \quad (s_{\max} \ll \langle s \rangle) \quad (1)$$

where $\langle s \rangle$ is the mean level spacing of the delocalized levels and s_{\max} is the window size (600 MHz, here). We predict that we should only observe a torsionally delocalized state in the IR spectrum 17% of the time. Even if the actual state density is a factor of 2 higher due to anharmonic corrections to the state count, we only expect a 33% chance of observing these states. A possible alternative explanation is that these transitions are actually cis-like vibrational states but originating from quantum states with several quanta of low-lying normal-mode vibrations. However, estimates of the shift in the transition frequency based on the average number of quanta in a typical bath state strongly fail to account for this difference.⁴² We conclude that these interactions do originate in coupling to vibrational states with torsionally delocalized character and that we have been fortunate to observe so many.

We have also detected the coupling to torsionally delocalized states in the gauche spectrum of allyl fluoride. A diagram of this measurement is shown in Figure 9. The observed transition frequencies are listed in Table 3. We have measured the rotational spectra of the three 1_{01} eigenstates with the largest infrared intensity. These eigenstates include the two closely spaced eigenstates near 0 MHz of the 1_{01} IVR multiplet seen in Figure 9, as well as the eigenstate that lies approximately 1700 MHz higher in energy. The higher energy 1_{01} eigenstate (near

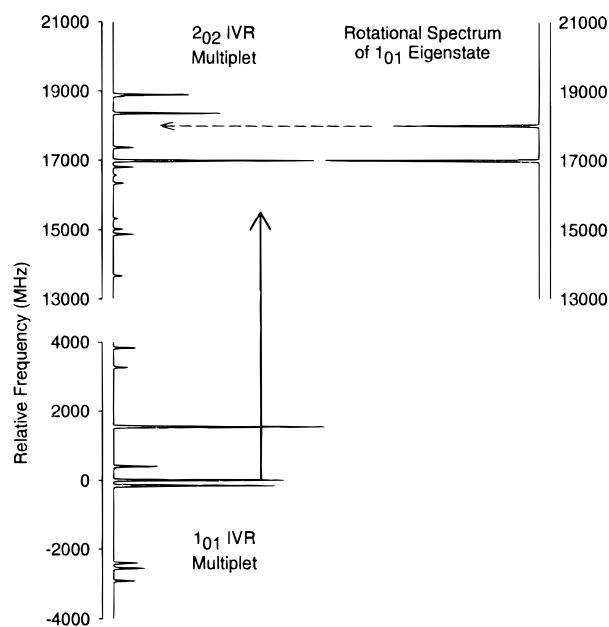


Figure 9. Shown here is a relative energy plot of the gauche 1_{01} and 2_{02} IVR multiplets. Also seen is the rotational spectrum of the indicated 1_{01} eigenstate, also on the same relative energy scale. The lower frequency transition accesses a 2_{02} eigenstate observed in the infrared spectrum. The higher frequency transition is assigned to a delocalized state transition. The $J = 2$ final state of the transition does not appear in the infrared spectrum.

1700 MHz on this relative scale) has two rotational transitions. These transitions access the two eigenstates of the 2_{02} multiplet seen with nearly equal intensity in the infrared spectrum near 19000 MHz and 18500 MHz on the relative frequency scale of Figure 9. These transition frequencies are consistent with transitions of states with delocalized character. The fact that these two eigenstates are accessed from the same initial state demonstrates that they belong to the same parity component of the IVR multiplet.²³ For each of the two 1_{01} eigenstates near 0 MHz on the relative frequency scale, we observe rotational transitions to the same two eigenstates. Both of these eigenstates lie higher in energy. One transition occurs near the expected $2_{02}-1_{01}$ transition frequency of the gauche conformer (16983 MHz and 17143 MHz for the two eigenstates) and one transition occurs at frequency similar to those assigned to delocalized torsional state transitions in the cis spectrum (17994 MHz and 18154 MHz).

By calibrating the IR spectra of the 1_{01} and 2_{02} IVR multiplets, we determine that the lower frequency transitions (16983 MHz and 17143 MHz) from the two 1_{01} eigenstates near 0 MHz reach the molecular eigenstate with the strongest intensity in the 2_{02} IVR multiplet. However, the other eigenstate accessed in the rotational transitions (17994 MHz and 18154 MHz) is unobservable in the IR spectrum, as seen in Figure 9. The spacing between the two equally intense 1_{01} eigenstates is 158 MHz. If we treat this interaction as an isolated two-state interaction then the matrix element for this coupling is 79 MHz.⁴³ With such a weak coupling between the gauche and delocalized states, this state does not participate in the coupling at $J = 2$ because there is no nearby gauche state for it to interact with. The matrix element for this gauche-delocalized interaction is of the same order as those observed for the cis-delocalized interactions.

Detection of Coupling to Vibrational States of the Other Conformer. We have looked for evidence of coupling between states with gauche and cis torsional character in both the IR spectrum of the cis and gauche conformers.^{19,22} For the cis

TABLE 4: Summary of Microwave Scans of the Gauche Allyl Fluoride Eigenstates of the Asymmetric CH₂ Ethylenic Stretch Vibrational Band

IVR Multiplet ($J_{K_a K_c}$)	frequency (cm ⁻¹)	frequency searched (GHz)	rotational transitions observed (MHz) ^a	attempted observation ($J'_{K'_a K'_c} \leftarrow J''_{K''_a K''_c}$, conformer)
1 ₀₁	3099.15	15.3–18.5	16807/17346	2 ₀₂ –1 ₀₁ , gauche
	3099.10	12–18.3	16983/17994	1 ₁₀ –1 ₀₁ , cis; 2 ₀₂ –1 ₀₁ , gauche
	3099.09	9.6–18.5	17143/18154	1 ₁₀ –1 ₀₁ , cis; 2 ₀₂ –1 ₀₁ , gauche
2 ₀₂	3099.12	15.3–18.5	17346	2 ₀₂ –1 ₀₁ , gauche
	3099.10	13.3–18.5	16807/17955	2 ₁₁ –2 ₀₂ cis; 2 ₀₂ –1 ₀₁ gauche
	3099.05	13.7–14.7	none observed	2 ₁₁ –2 ₀₂ , cis
3 ₀₃	3098.82	15–18.2	none observed	3 ₁₂ –3 ₀₃ , cis
	3098.79	15–18.3	none observed	3 ₁₂ –3 ₀₃ , cis
3 ₁₂ ^b	3100.70 ⁻	15.3–18.5	none observed	3 ₁₂ –3 ₀₃ , cis
	3100.69 ⁺	15.3–18.5	none observed	3 ₁₂ –3 ₀₃ , cis
	3100.69 ⁺	15.3–18.5	none observed	3 ₁₂ –3 ₀₃ , cis
	3100.67 ⁻	15.3–18.5	none observed	3 ₁₂ –3 ₀₃ , cis

^a Assignments are given in Table 3. ^b The + or – designates the parity of the eigenstate.

spectrum, we expect that coupling to a state with gauche character would have produced rotational transitions near 16.8 GHz for the $J = 2-1$ rotational spectrum. Although we found several instances of coupling to delocalized torsional states in these measurements, we were unable to detect any gauche-like transitions. For the gauche IR spectrum, we have looked for $K_a = 1-0$ b-type Q-branch transitions at the characteristic cis rotational frequencies. We have investigated eigenstates in the $J = 0-3$, $K_a = 0,1$ IVR multiplets of the gauche conformer. A summary of these searches is given in Table 4. Again, we have found no evidence of coupling to states of the other conformer. For the level densities found in this spectrum we expect that the rotational spectra will show complementarity and that the eigenstates with weak IR intensity are most likely to show rotational transitions of the other conformer.¹⁸ The weakness of the gauche IR spectrum has prevented us from measuring the rotational spectra of these eigenstates.⁴⁴ We conclude that “isomerization” does not occur in the cis spectrum and is at best a slow, local phenomenon in the gauche spectrum. Similar conclusions were drawn about the lack of significant direct gauche-cis coupling from the analysis of the calculated versus observed state density of the gauche infrared spectrum.²³

Conclusions

By measuring the rotational spectra of single molecular eigenstates in the asymmetric =CH₂ stretch spectrum of the cis and gauche allyl fluoride conformers we have been able to characterize the weak vibrational coupling mechanisms. In the analysis of the cis IR spectrum, we proposed that the weak interactions found in the spectrum were caused by either Coriolis interactions or coupling to vibrational states with either gauche or delocalized torsional character.²³ For all of the cis spectra we have investigated we are able to demonstrate that these weak interactions are caused by Coriolis coupling (the 3₂₁ IVR multiplet) or coupling to torsionally delocalized states (the $J = 1$ and $J = 2$ IVR multiplets). In both cases, the matrix elements are weak and on the order of 80 MHz. This similarity of the matrix elements suggests a common origin for these interactions. The presence of an internal rotor in the molecule generates terms in the Hamiltonian that can be interpreted as Coriolis-like interactions^{30,35,45,46} (additionally there are centrifugal terms that can be attributed to “axis switching” effects⁴⁵). Therefore, the coupling to the torsionally delocalized states may also be caused by a Coriolis mechanism.

In the gauche IR spectrum, we have also observed interactions with torsionally delocalized states. The interaction matrix element for the gauche-delocalized coupling is of the same magnitude as found for the cis-delocalized interactions. In

neither the cis nor the gauche spectrum have we found evidence for direct coupling between the two conformers. We believe this result indicates that conformational isomerization, defined as coupling between states with cis and gauche torsional character, is mediated by the delocalized torsional states (also called “isomerization states”).^{19,47} For example, in the region of the cis asymmetric =CH₂ stretch, the density of gauche-like states is 3.6 times greater than the density of delocalized states.²³ If the direct interaction between the cis bright-state and the gauche bath states were as strong as the cis-delocalized interactions, then we would have been about four times more likely to observe gauche rotational transitions. The torsionally delocalized states behave as “doorway” states to the isomerization process.⁴⁷ The weak coupling to these isomerization states, compared to coupling between vibrational states of the same torsional character, leads to a situation where the IVR dynamics are expected to show two distinct time scales: rapid IVR with retention of conformation followed by a slower conformational isomerization process. As was pointed out in the previous paper, the isomerization rates are orders-of-magnitude slower than predicted by RRKM theory.²³ The bottleneck to the isomerization process appears to be the slow rate for reaching the torsionally delocalized states.^{48,49}

Finally, we note that the highly torsionally excited states do not appear to show significantly faster IVR. This conclusion is inferred from the simplicity of the rotational spectra that we observe. For example, in the cis spectrum, the rotational spectra of the torsionally delocalized states show either one or two transitions. This observation indicates limited IVR of this coupled state. Similarly, a simple rotational spectrum is observed for the torsionally delocalized state in the gauche spectrum. The weak coupling of these free-rotor-like states to the states of well-defined conformational character (e.g., cis or gauche) may have a similar origin as the narrowing found in the spectra of “extreme motion” vibrational states.^{50,51} If the weak interactions persist to higher energies, then it will be generally true that conformational isomerization is a slow dynamical process in large polyatomic molecules.

Acknowledgment. This work has been supported by the National Science Foundation through CAREER Award CHE-9624850. Support has also been provided by the Jeffress Trust. David A. McWhorter acknowledges support from a Presidential Fellowship from the University of Virginia.

References and Notes

- (1) Robinson, P. J.; Holbrook, K. A. *Unimolecular Reactions*; Wiley-Interscience: New York, 1972.

- (2) Baer, T.; Hase, W. L. *Unimolecular Reaction Dynamics, Theory and Experiment*; Oxford University Press: New York, 1996.
- (3) Leinau, C.; Heikal, A. A.; Zewail, A. H. *Chem. Phys.* **1993**, *175*, 171.
- (4) Hamm, P.; Lim, M.; Hochstrasser, R. M. *J. Chem. Phys.* **1997**, *107*, 10523.
- (5) Arrivo, S. M.; Heilweil, E. J. *J. Phys. Chem.* **1996**, *100*, 11975.
- (6) Perry, D. S. *J. Chem. Phys.* **1993**, *98*, 6665.
- (7) McLroy, A.; Nesbitt, D. J. *J. Chem. Phys.* **1990**, *92*, 2229.
- (8) Pate, B. H.; Lehmann, K. K.; Scoles, G. *J. Chem. Phys.* **1991**, *95*, 3891.
- (9) Fraser, G. T.; Pate, B. H.; Bethardy, G. A.; Perry, D. S. *J. Chem. Phys.* **1993**, *175*, 223.
- (10) Kommandeur, J.; Majewski, W. A.; Meerts, W. L.; Pratt, D. W. *Annu. Rev. Phys. Chem.* **1987**, *38*, 443.
- (11) Elsaesser, T.; Kaiser, W. *Annu. Rev. Phys. Chem.* **1991**, *42*, 83.
- (12) Ambroseo, J. R.; Hochstrasser, R. M. *J. Chem. Phys.* **1988**, *89*, 5956.
- (13) Reid, P. J.; Diog, S. J.; Wickham, S. D.; Mathies, R. A. *J. Am. Chem. Soc.* **1993**, *115*, 4754.
- (14) Minton, T. K.; Kim, H. L.; Reid, S. A.; McDonald, J. D. *J. Chem. Phys.* **1988**, *89*, 6550.
- (15) Boyarkin, O. V.; Lubich, L.; Settle, R. D. F.; Perry, D. S.; Rizzo, T. R. *J. Chem. Phys.* **1997**, *104*, 8409.
- (16) Pate, B. H. *J. Chem. Phys.* **1998**, *109*, 4396.
- (17) Green, D.; Holmberg, R.; Lee, C. Y.; McWhorter, D. A.; Pate, B. H., *J. Chem. Phys.* **1998**, *109*, 4407.
- (18) Pate, B. H. *J. Chem. Phys.* Submitted for publication.
- (19) McWhorter, D. A.; Hudspeth, E.; Pate, B. H. *J. Chem. Phys.* Submitted for publication.
- (20) Gunther, H. *NMR Spectroscopy, Second Edition*; John Wiley and Sons: New York, 1995.
- (21) Slichter, C. P. *Principles of Magnetic Resonance*; Springer-Verlag: New York, 1980.
- (22) Hudspeth, E.; McWhorter, D. A.; Pate, B. H. *J. Chem. Phys.* **1997**, *107*, 8189.
- (23) McWhorter, D. A.; Pate, B. H. *J. Phys. Chem. A* **1998**, *102*, 8786.
- (24) Lehmann, K. K.; Scoles, G.; Pate, B. H. *Annu. Rev. Phys. Chem.* **1994**, *45*, 241.
- (25) Nesbit, D. J.; Field, R. W. *J. Phys. Chem.* **1996**, *100*, 12735.
- (26) Aulter, S. H.; Townes, C. H. *Physical Review*. **1955**, *100*, 703.
- (27) Gordy, W.; Cook, R. L. *Microwave Molecular Spectra*; John Wiley & Sons: New York, 1984.
- (28) Gaussian 94 (Revision D.1), Frisch M. J.; Trucks G. W.; Schlegel H. B.; Gill P. M. W.; Johnson B. G.; Robb M. A.; Cheeseman J. R.; Keith T. A.; Petersson G. A.; Montgomery J. A.; Ragavachari K.; Al-Laham M. A.; Karkzewski V. G.; Ortiz J. V.; Foresman J. B.; Cioslowski J.; Stefanov B. B.; Nanayakkara A.; Challacombe M.; Peng C. Y.; Ayala P. Y.; Chen W.; Wong M. W.; Andres J. L.; Replogle E. S.; Gomperts R.; Martin R. L.; Fox D. J.; Binkley J. S.; Defrees D. J.; Baker J.; Stewart J. P.; Head-Gordon M.; Gonzales C.; Pople J. A.; Gaussian, Inc., Pittsburgh, PA, 1995.
- (29) Luppi, J.; Rasanen, M.; Murto, J.; Pajunen, P. *J. Mol. Struct.* **1991**, *245*, 307.
- (30) Meakin, P.; Harris, D. O.; Hirota, E. *J. Chem. Phys.* **1969**, *51*, 3775.
- (31) Durig, J. R.; Zhen, M.; Little, T. S. *J. Chem. Phys.* **1984**, *81*, 4259.
- (32) Lewis, J. D.; Mallory, T. B.; Chao, T. H.; Laane, J. *J. Mol. Struct.* **1972**, *12*, 427.
- (33) Pitzer, K. S. *J. Chem. Phys.* **1946**, *14*, 239.
- (34) D. A. McWhorter, Ph.D. Thesis, University of Virginia, August, 1998 (Chapter 3).
- (35) Meyer, R.; Wilson, E. B. *J. Chem. Phys.* **1970**, *53*, 3969.
- (36) Hirota, E. *J. Chem. Phys.* **1965**, *42*, 2071.
- (37) Because there are so few states involved in the vibrational mixing in the cis vibrational band, we expect to be able to interpret these spectra approximately as two-state interactions similar to those seen in: Miller, C. C.; Philips, L. A.; Andrews, A. M.; Fraser, G. T.; Pate, B. H.; Suenram, R. D. *J. Chem. Phys.* **1994**, *100*, 831. Ainetshian, A.; Fraser, G. T.; Pate, B. H.; Suenram, R. D. *Chem. Phys.* **1995**, *190*, 231.
- (38) Hudspeth, E.; McWhorter, D. A.; Pate, B. H. *J. Chem. Phys.* **1998**, *109*, 4316.
- (39) Lawrance, W. D.; Knight, A. E. W. *J. Phys. Chem.* **1985**, *89*, 917.
- (40) Lehmann, K. K. *J. Phys. Chem.* **1991**, *95*, 7556.
- (41) We have calibrated the electric field strength of our microwave radiation (50 V/cm) and expect that a rotational transition strength of 0.1 D would result in a 2.5 MHz line width for saturation spectroscopy.
- (42) The rotational constants for gauche allyl fluoride in the first excited state of the skeletal bending vibration have been reported by Hirota (ref 35). If one assumes that the shift in rotational constants for the cis conformer is similar, then for each quanta of torsional energy in this mode, there is a decrease in (B+C) of 30 MHz. Even if all 3000 cm⁻¹ of energy were localized in this torsional motion, the 2₀₂-1₀₁ cis rotational transition would only be shifted by ~600 MHz from the ground-state value. The transitions we observe and assign to delocalized state transitions differ from the ground state cis rotational frequency by about 3 GHz. Furthermore, the skeletal torsion mode has rotational constants smaller than the rotational constants for the gauche conformer. Therefore, any rotational transition from an eigenstate of the gauche vibrational band that is due to contribution from these states, would fall to lower frequency than the ground state gauche transition, farther from the observed frequencies that we assign to delocalized transitions.
- (43) Although we have treated this as a two state interaction, the delocalized state is actually interacting with a state of "premixed" gauche character. For a discussion of this idea, see: Green, D.; Hammond, S.; Keske, J.; Pate, B. H. *J. Chem. Phys.* Submitted for publication.
- (44) Although saturation of the eigenstates is not a requirement, the intensity of the infrared transition must be sufficiently strong such that we are able to achieve a stable lock on the infrared transition.
- (45) Quade, C. R.; Lin, C. C. *J. Chem. Phys.* **1963**, *38*, 540.
- (46) Li, H.; Ezra, G. S.; Philips, L. A. *J. Chem. Phys.* **1992**, *97*, 5956.
- (47) Bowman, J. M.; Gazdy, B. *J. Phys. Chem. A* **1997**, *101*, 6384.
- (48) Leitner, D. M.; Wolynes, P. G. *Chem. Phys. Lett.* **1997**, *280*, 411.
- (49) Borchardt, D. B.; Bauer, S. H. *J. Chem. Phys.* **1986**, *85*, 4980.
- (50) Choi, Y. S.; Moore, C. B. *J. Chem. Phys.* **1991**, *94*, 5414.
- (51) Hose, G.; Taylor, H. S. *Chem. Phys.* **1984**, *84*, 375.